Coastal Louisiana landscape and storm surge evolution: 1850–2110

Christopher G. Siverd, Scott C. Hagen, Matthew V. Bilskie, DeWitt H. Braud, R. Hampton Peele, Madeline R. Foster-Martinez, et al.

Climatic Change
An Interdisciplinary, International Journal Devoted to the Description, Causes and Implications of Climatic Change

ISSN 0165-0009

Climatic Change
DOI 10.1007/s10584-019-02575-7

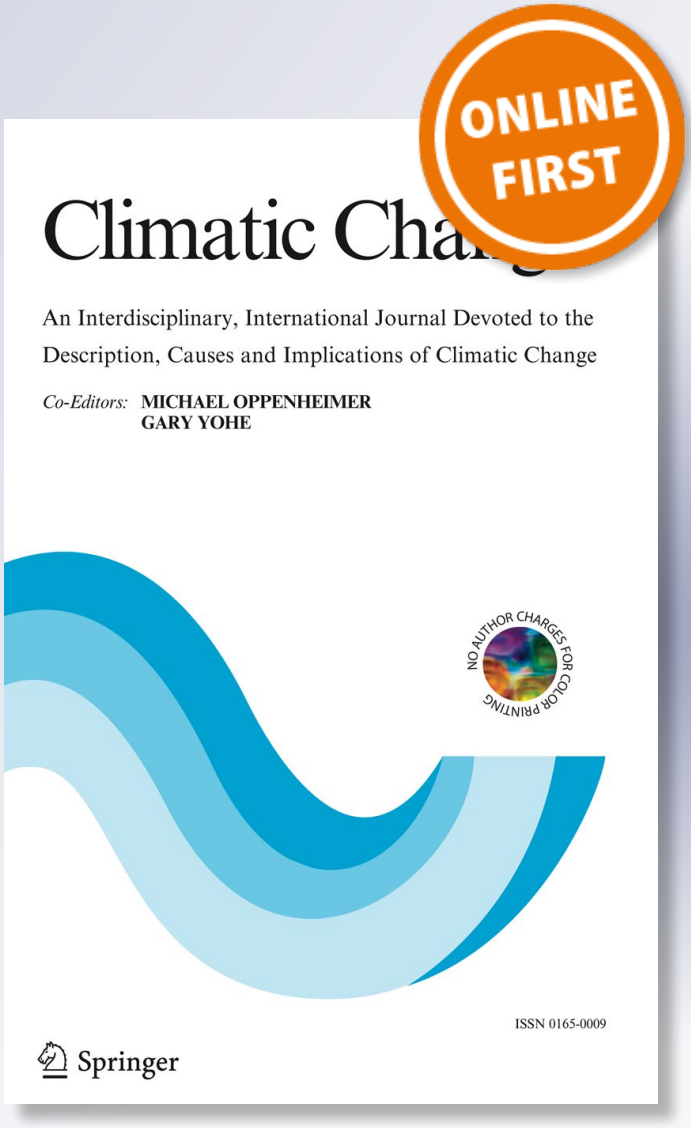

Springer

Climatic Change
https://doi.org/10.1007/s10584-019-02575-7

Coastal Louisiana landscape and storm surge evolution: 1850–2110

Christopher G. Siverd[1] · Scott C. Hagen[1,2,3,4] · Matthew V. Bilskie[2] · DeWitt H. Braud[4] · R. Hampton Peele[5] · Madeline R. Foster-Martinez[2] · Robert R. Twilley[4,6]

Received: 30 April 2019 / Accepted: 2 October 2019/Published online: 27 November 2019

Abstract

Storm surge models are constructed to represent the Louisiana coastal landscape circa 1850, 1890, 1930, 1970, 1990, 2010, 2030, 2050, 2070, 2090, and 2110. Historical maps are utilized to develop models with past landscapes while a continuation of recent landscape trends is assumed for future models. The same suite of meteorological wind and pressure fields is simulated with each storm surge model. Simulation results for 1850 and 1890 demonstrate minimal change in storm surge characteristics along the Louisiana coast. A mean maximum storm surge height increase of 0.26 m from 1930 to 2010 is quantified within the sediment-abundant Atchafalaya-Vermilion coastal basin, while increases of 0.34 m and 0.41 m are quantified within sediment-starved Terrebonne and Barataria, respectively. Future mean maximum storm surge heights increase across these three coastal basins by 0.67 m, 0.55 m, and 0.75 m, indicating negligible differences from 2010 to 2110, regardless of sediment availability. Results indicate that past changes in the Louisiana coastal landscape and storm surge were a consequence of local land and river management decisions while future changes are dominated by relative (subsidence and eustatic) sea level rise. Projecting landscape and surge changes beyond 50 years could aide policy makers as they work to enhance resilience across coastal Louisiana. Similar analyses could be conducted for other deltas across the world, such as the Ganges, that are experiencing challenges comparable to those of the Mississippi River Delta.

Keywords Wetland loss · Land water ratio · ADCIRC · Coastal flood risk · Hydrologic unit code · Storm surge

Electronic supplementary material The online version of this article (https://doi.org/10.1007/s10584-019-02575-7) contains supplementary material, which is available to authorized users.

✉ Christopher G. Siverd
cg.siverd@gmail.com

Extended author information available on the last page of the article

1 Introduction

Deltas across the world are drowning due to relative sea level rise (sum of local subsidence and local eustatic sea level rise), which has major implications for humans and ecosystems that depend on their existence (Kulp and Strauss 2017; Syvitski et al. 2009; Vörösmarty et al. 2009; Wong et al. 2017). Syvitski et al. (2009) grouped 33 major deltas by risk of substantial change throughout the twenty-first century due to relative sea level rise. The Ganges, Irrawaddy, Magdalena, Mekong, Mississippi, Niger, and Tigris all feature relative sea level rise rates greater than that of global mean sea level (GMSL) rise. The Ganges and Mississippi Deltas are especially similar in terms of areas susceptible to storm surge and historical rates of aggradation and relative sea level rise (Syvitski et al. 2009). In the Mississippi Delta, river management decisions have increased the magnitude of relative sea level rise during the last century (Blum and Roberts 2009; Day Jr. et al. 2007; Twilley et al. 2016). Levee construction and the closing of Mississippi River distributaries have resulted in wetland loss and increased inland storm surge heights across Louisiana hydrologic coastal basins with substantially reduced riverine sediment input (i.e., sediment-starved). In contrast, minor landscape changes have occurred in the Atchafalaya-Vermilion hydrologic coastal basin with continued riverine sediment input (i.e., sediment abundant) (Siverd et al. 2019, 2018). Deltas and their inhabitants will continue to be stressed as annual rates of GMSL rise are projected to increase throughout the twenty-first century with extreme scenarios ranging from 1.0 to 2.5 m (Jevrejeva et al. 2016; Stocker et al. 2013; Sweet et al. 2017). The goal of this analysis is to quantify the change in storm surge characteristics from 1850 to 2110 across coastal Louisiana due to landscape changes and eustatic sea level rise via a methodology that could be applied to similar deltas across the world such as the Ganges.

During the past few decades, numerical storm surge model development focused on accurately representing landscape features to produce more accurate results (Ali 1999; Bilskie et al. 2015; Bilskie and Hagen 2013; Bilskie et al. 2016b; Blain et al. 1998; Dietrich et al. 2011a; Lawler et al. 2016; Luettich and Westerink 2004; Massey et al. 2015; Massey et al. 2011; Walstra et al. 2012; Westerink et al. 2008). Recent studies have also examined the impact of modern hurricanes on past landscapes (Irish et al. 2013) and the nonlinear response of storm surge to GMSL rise (Atkinson et al. 2012; Bilskie et al. 2016a; Bilskie et al. 2019; Bilskie et al. 2014; Smith et al. 2010). Land to water (L:W) isopleths are lines that connect areas of the same percentage of land with respect to water along the Louisiana coast and were previously derived from satellite imagery and historical maps. L:W isopleths were previously utilized to simplify a detailed modern-day Louisiana coastal landscape with coastal zones labeled high (99% through 90% L:W isopleths), intermediate (90–40%), and submersed (40–1%) most closely reproducing the detailed coastal Louisiana landscape. For more details, see Siverd et al. (2018, 2019) and Twilley et al. (2016). In this analysis, L:W isopleths with the same percentage of land with respect to water (90%, 40%, and 1%) derived circa 1850, 1890, 1930, 1970, 1990, 2010, 2030, 2050, 2070, 2090, and 2110 are applied in storm surge model mesh development and serve as a connector of temporal wetland loss and storm surge evolution from 1850 to 2110. Simple landscape representations of the Louisiana coast are developed for each mesh year due to the lack of comparable topo-bathymetry prior to the early 2000s (Siverd et al. 2018).

The aim of this analysis is to quantify the historical and future evolution of storm surge across the Louisiana coastal landscape from 1850 to 2110. Storm surge characteristics such as maximum water surface elevations, storm surge inundation time, and maximum significant

wave heights are quantified, and difference plots are generated. The impact of coastal deforestation on storm surge is also examined. Future Louisiana coastal landscapes are qualitatively compared with the projections of the Louisiana Coastal Wetlands Conservation and Restoration Task Force (1993), Barras et al. (2003), and the 2017 Louisiana Coastal Protection and Restoration Authority (CPRA) coastal masterplan. Storm surge maximum water surface elevations and maximum significant wave height results are included in the main text. Inundation time results and the coastal deforestation analysis reinforce conclusions drawn from analyzing maximum water surface elevation and maximum significant waves and are included in Online Resource 1. Resio and Westerink (2008) issued a challenge to develop storm surge models that could be used to design flood defenses through an approach that "looks far into the future." In this analysis, we provide an approach to address this challenge.

2 Study area

The study area is the Louisiana coast, which is bound by Sabine Lake (west), Pearl River (east), Intracoastal Waterway (ICWW) (north), and the Gulf of Mexico (GOM) (south) (Fig. 1). The Louisiana coast is characterized by small topographic gradients, numerous man-made canals, and navigation waterways. The study area has changed substantially since 1850. In the nineteenth century, coastal forests were harvested for lumber (Fig. 2) (Conner and Toliver 1990). In both the nineteenth and twentieth centuries, levees were constructed adjacent to the Mississippi River for flood control (U.S. Army Corps of Engineers 2016). Throughout the twentieth century, 16,853 km of petroleum canals was excavated in addition to numerous wide and deep navigation waterways (Turner and McClenachan 2018). By 2010, 4877 km^2 of Louisiana coastal wetlands and barrier islands was lost due to changes in river management, subsidence caused by lack of sediment deposition subsequent to the channeling of the Mississippi River, and compaction due to subsurface mining (hydrocarbon and groundwater) (Blum and Roberts 2009; Nienhuis et al. 2017; Syvitski et al. 2009), and eustatic (including seasonal GOM expansion) sea level rise, with eustatic sea level rise providing only a minimal historical contribution (Fig. 2) (Batker et al. 2010; Couvillion et al. 2011; Siverd et al. 2019). This analysis utilizes observed historical GMSL rise measurements and a conservative future GMSL rise scenario to determine the initial GOM water level for each storm surge model year 1850 through 2110. See Online Resource 1 for more details regarding the study area.

3 Methods

3.1 Hydrodynamic model and mesh development of historical landscapes

Storm surge simulations are facilitated through application of a coupled ADvanced CIRCulation two-dimensional depth-integrated (ADCIRC-2DDI) code (Luettich Jr. et al. 1992) and the third-generation wave model Simulating WAves Nearshore (SWAN) (Booij et al. 1999; Dietrich et al. 2011b; Zijlema 2010). ADCIRC solves the depth-averaged shallow water equations (SWEs) for water surface elevations and depth-averaged currents, and SWAN computes the wave action density spectrum (Dietrich et al. 2011b). Wind, pressure, and wave forcings are included in this analysis, while tide and river discharge forcings are excluded to reduce complexity and because the latter have only minor influence on surge results (National Oceanic and Atmospheric Administration 2018).

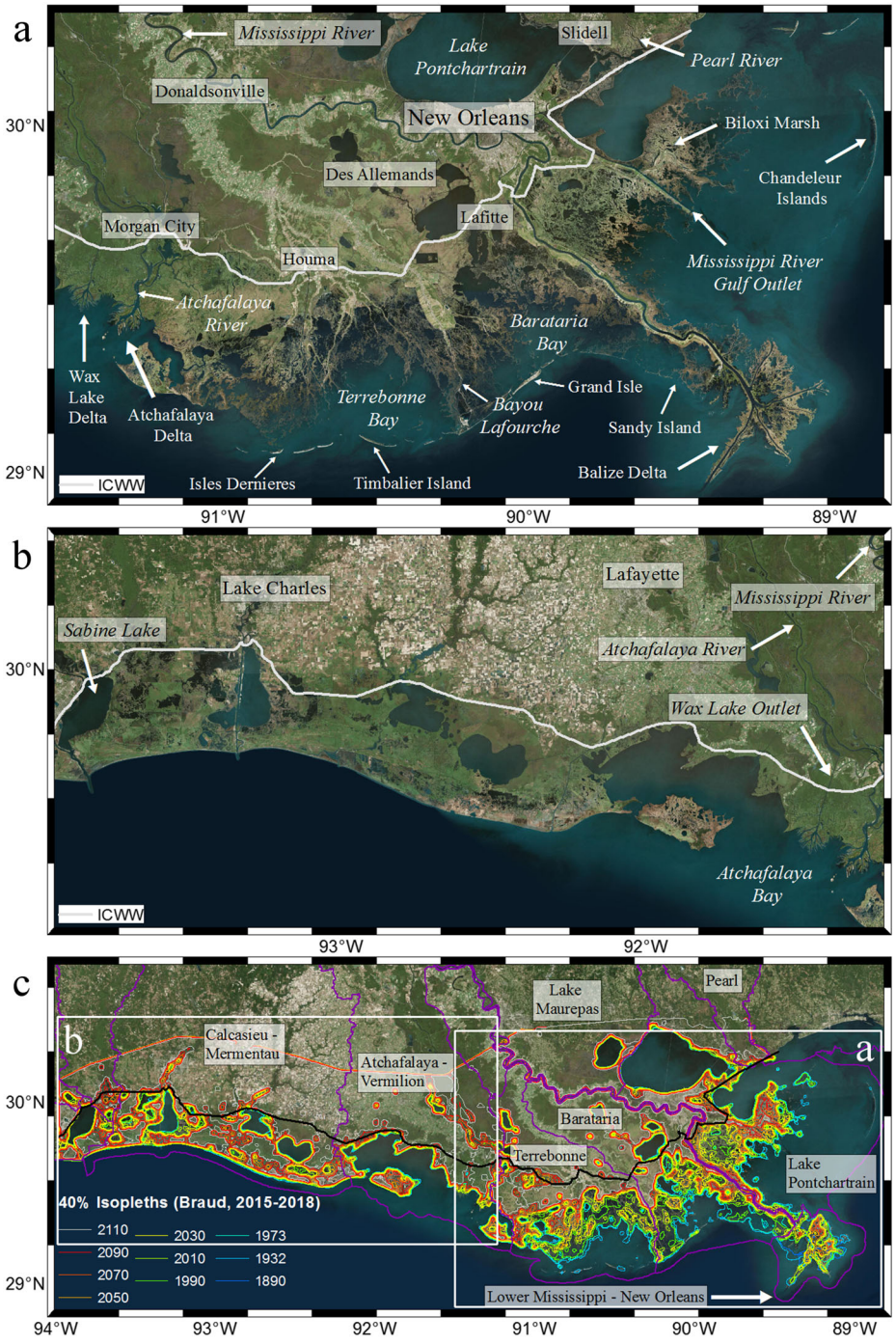

Fig. 1 Year 2015 and 2016 satellite images. **a** Major coastal features and cities of southeast Louisiana. **b** Major coastal features and cities of southwest Louisiana. **c** 40% L:W isopleths for years 1890, 1932, 1973, 1990, 2010, 2030, 2050, 2070, 2090, and 2110. Black line indicates the Intracoastal Waterway (ICWW). Purple lines indicate hydrologic unit code 6 (HUC6) coastal basins

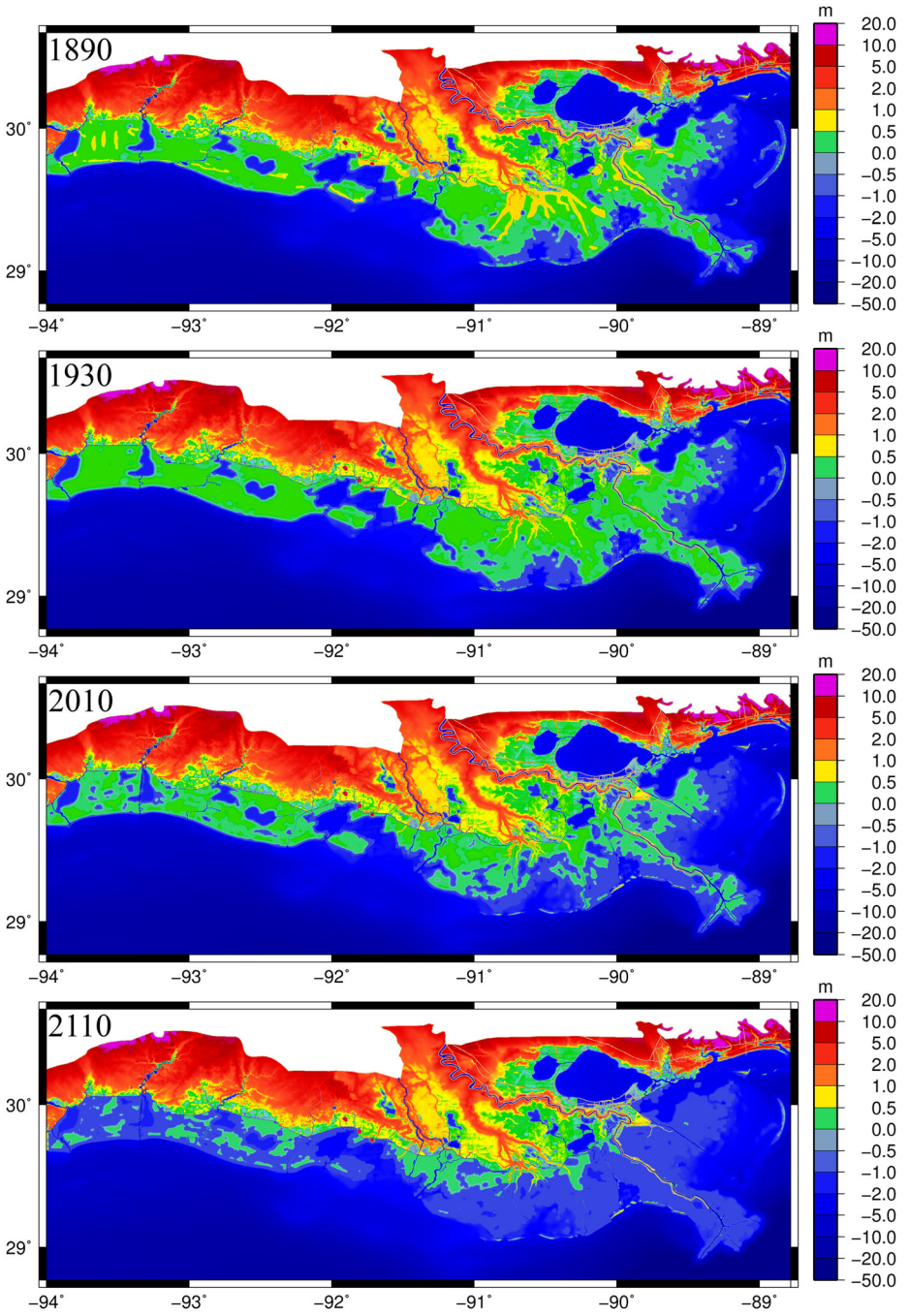

Fig. 2 Topography and bathymetry: 1890, 1930, 2010, and 2110

An approach is developed to construct numerical storm surge models featuring both historical and future landscapes of the Louisiana coast. A storm surge model mesh is a

topological network comprising elements and nodes containing elevation data. The mesh developed for the 2017 CPRA Louisiana Coastal Master Plan (Fischbach et al. 2017) serves as a base to edit and construct meshes featuring the Louisiana coastal landscape circa 1850, 1890, 1930, 1970, 1990, 2010, 2030, 2050, 2070, 2090, and 2110. The CPRA2017 base mesh features approximately 1.4 million nodes and 2.7 million elements. The base mesh focuses on the Louisiana coast with 93% of nodes between Mobile Bay, Alabama, and the Bolivar Peninsula, Texas, and describes the western north Atlantic Ocean west of the 60° W meridian, GOM, and Caribbean Sea. Because only Mississippi River levees existed in 1850, man-made features such as levees are removed from the CPRA2017 mesh south and west of the Mississippi River to compare changes in storm surge characteristics due to land loss across all mesh years from 1850 to 2110. Removing levees in the study area also removes the need to account for future levee construction or abandonment (see Siverd et al. (2018) for more details). Mesh resolution is enhanced seaward of the current (2019) barrier islands to accurately describe barrier islands in southeast Louisiana from 1850 to 2110. This modified CPRA2017 mesh is hereafter called the "detailed" storm surge model mesh.

Coastal zones are established via the position of the 90%, 40%, and 1% L:W isopleths along the Louisiana coast in the following configuration: high (ICWW—90%), intermediate (90–40%), and submersed (40–1%) (Siverd et al. 2018). Mesh nodes are assigned an elevation value (NAVD88) based on their respective zone classification, high, 0.47 m; intermediate, 0.27 m; and submersed, − 0.98 m. Manning's n bottom roughness values are also assigned per coastal zone, high, 0.070; intermediate, 0.045; and submersed, 0.025. In accordance with Church et al. (2013), historical GOM initial water levels are set for each storm surge model based on the following GMSL rise rates: 0.5 mm/year 1850–1890, 1.0 mm/year 1890–1930, 2.0 mm/year 1930–2010. The Intermediate-Low scenario from Sweet et al. (2017), which averages 5.1 mm/year 2010–2110 (Table 1), is selected for future models. GOM initial water levels are derived from the 2010 starting point of 0.23 m NAVD88, which was established by the U.S. Army Corps Joint Storm Surge (JSS) study and describes the annual summer increase in GOM water levels (U.S. Army Corps of Engineers 2008). To further explain, historical water levels are set by subtracting the GMSL rise between each historical model year and the 2010 starting value of 0.23 m NAVD88. Future initial water levels are set by adding the Intermediate-Low projected rise in sea levels to the 2010 value of 0.23-m NAVD88 for each model year (Table 1).

3.1.1 Storm surge model meshes

For the 1850, 1890, 1930, 1970, 1990, and 2010 storm surge model meshes, the location of the Intracoastal Waterway (ICWW) is designated the northern boundary of the study area even though excavation did not begin until 1925 (Fig. 1c) (Harrison 2015). Because data exist, barrier islands from Isles Dernieres to the Chandeleur Islands are input according to U.S. Coast and Geodetic Survey (USC&GS) T-Sheets and the USGS 1:62.5k quads for 1850 and 1890 (Supplementary Table 1). L:W isopleths (1%, 40%, 90%) were previously derived for 1932, 1973, 1990, and 2010 and applied to the detailed model mesh from Lake Sabine to the Pearl River to construct meshes circa 1930, 1970, 1990, and 2010 (Fig. 2). USGS quad sheets and/or National Oceanic and Atmospheric Administration (NOAA) T-sheets were utilized to input barrier islands, ridges, and navigation waterways as they existed in each mesh year. For more details regarding mesh years 1930, 1970, and 2010, see Siverd et al. (2019). For mesh years 1850, 1890, and 1990, see Online Resource 1.

Table 1 Storm surge model descriptions. 1890 wooded areas are inserted in model 12 for the sensitivity analysis

No.	Storm surge model mesh (year)	GOM initial water level (m)	Navigation waterways (year)	Surface canopy (year)	Surface directional roughness (z0) (year)
Historical and future storm surge models					
1	1850	0.01	1850	1850–1890	1850–1890
2	1890	0.03	1890	1850–1890	1850–1890
3	1930	0.07	1930	1930–2110	1930–2110
4	1970	0.15	1970–2110	1930–2110	1930–2110
5	1990	0.19	1970–2110	1930–2110	1930–2110
6	2010	0.23	1970–2110	1930–2110	1930–2110
7	2030	0.32	1970–2110	1930–2110	1930–2110
8	2050	0.43	1970–2110	1930–2110	1930–2110
9	2070	0.54	1970–2110	1930–2110	1930–2110
10	2090	0.64	1970–2110	1930–2110	1930–2110
11	2110	0.74	1970–2110	1930–2110	1930–2110
Sensitivity analysis storm surge model					
12	2010	0.23	1970–2110	1850–1890	1850-1890

3.2 Hydrodynamic model mesh development of future landscapes

Recall that the 1% L:W isopleth indicates one part land for every 100 parts water, or virtually open water. For all historical storm surge models (1850–2010), the position of the 1% L:W isopleth demonstrates only minor spatial variations due to the CPRA's recent restoration of the barrier islands. Additionally, the CPRA has committed to maintaining the barrier islands through a periodic rebuilding campaign (Coastal Protection and Restoration Authority 2018). Therefore, the 2010 1% L:W isopleth is utilized for the location of the 1% L:W isopleth for all meshes featuring future Louisiana landscapes. Conversely, a trend in isopleth migration is observed across storm surge model mesh years 1970, 1990, and 2010 for interior L:W isopleths. The land to water ratio decreases by approximately 10% at all locations south of the ICWW for each 20-year interval with only minor variations (i.e., the 40% L:W isopleth in 1970 converts to 30% in 1990 and 20% in 2010). This trend is extrapolated into the future using the 2010 L:W isopleths: the 2010 50% L:W isopleth is considered spatially equal to the 2030 40%; 2010 60% equals 2050 40%; 2010 70% equals 2070 40%, 2010 80% equals 2090 40%, and 2010 90% equals 2110 40% (Fig. 1c). Similarly, 2010 99% equals the 2030 90%. Because L:W isopleth migration trends of the recent past are assumed to continue into the future, substantial increases or decreases in annual subsidence rates are assumed not to occur.

The only exception to the land loss trend is in the Wax Lake-Atchafalaya Deltas where land has been increasing since 1970. According to Wells et al. (1984) and Twilley et al. (2008), a delta rapidly grows for the first 60 to 90 years after the initial emergence of land. Subsequent delta growth slows substantially due to radial expansion assuming constant sediment supply, subsidence, and erosion rates. The Wax Lake Outlet was dredged in the 1930s to reduce river flood risk in Morgan City, marking the beginning of the Wax Lake-Atchafalaya Delta formation (U.S. Geological Survey 2017b). Additionally, since 1970, the sediment loads of the Mississippi and Atchafalaya Rivers have decreased by approximately half (Blum and Roberts 2009; Siverd et al. 2019). Because the rapid growth phase of the Wax Lake-Atchafalaya Deltas has ended, sediment supply used to build the deltas has decreased by half and due to the projected future increase in annual GMSL rise, limited future delta growth is

assumed. Therefore, the 2010 40% L:W isopleth is utilized to input the position of the Wax Lake and Atchafalaya Deltas for 2030, 2050, 2070, 2090, and 2110.

The state of Louisiana has committed to rebuilding and maintaining the barrier islands from Isles Dernieres to the Chandeleur Islands (Coastal Protection and Restoration Authority 2017). Therefore, the barrier islands are assumed to stay in the same position far into the future. This is considered a conservative assumption because higher inland storm surge could occur if the barrier islands are not continuously rebuilt (Ulm et al. 2016). Barrier island position, elevation, and Manning's *n* values as they exist in the detailed model mesh are included in future meshes 2030 to 2110. For comparability purposes, the ICWW is maintained as the northern boundary of the study area even though landscape changes north of the ICWW are likely to occur but are unlikely to alter the response of storm surge flooding south of the ICWW. Future representations of the Louisiana coastal landscape from 2030 to 2110 portray a conservative scenario for the state of Louisiana because it is not known how areas susceptible to change such as the upper Atchafalaya-Vermilion, Terrebonne, Barataria coastal basins, land bridge between New Orleans East and Slidell, and the shoreline of Lake Pontchartrain will be maintained by the state and federal governments. Therefore, the elevation and Manning's *n* values north of the ICWW are unchanged through 2110. Future Louisiana coastal landscapes and surge results can also be considered conservative due to the extrapolation of the observed rate of land change between 1970 and 2010 to create the landscapes of 2030 through 2110 and due to the application of the NOAA Intermediate-Low future GMSL rise scenario to future model initial GOM water levels. Therefore, the impact of future increases in the rate of global ice melt is not included in this analysis.

3.3 Subsidence

Subsidence is addressed via the migration of the L:W isopleths inland from 1850 to 2110. Coastal zones high, intermediate, and submersed, which are delineated by the position of L:W isopleths, feature the same elevation and Manning's *n* values for all mesh years. As the 90% and 40% L:W isopleths migrate inland from 1850 to 2110, coastal zone high converts to intermediate and submersed thereby decreasing 9840 km^2 (100%), intermediate decreases 3746 km^2 (50%), and submersed doubles in size increasing by 11,913 km^2 (204%) (Fig. 3). Additionally, the 2010 average elevations derived for each coastal zone (Siverd et al. 2018) are supported via marsh elevations measured by Day et al. (2011).

3.4 Storm surge model simulations

The objective of this analysis is to quantify temporal changes in hurricane storm surge along the Louisiana coast due to landscape changes and eustatic sea level rise. To permit a reasonable comparison, all storm surge models are forced with the same suite of meteorological wind and pressure fields developed from 14 historical hurricanes (Cox et al. 1995; Powell et al. 1998). These 14 hurricanes include Isaac (2012), Gustav (2008), Ike (2008), Dennis (2005), Katrina (2005), Rita (2005), Ivan (2004), Georges (1998), Earl (1998), Opal (1995), Andrew (1992), Kate (1985), Elena (1985), and Agnes (1972) (Siverd et al. 2019). Simulated hurricane storm surges are from hurricanes that tracked across the GOM, reached category 1 status while in the GOM, and made landfall between Galveston and Apalachicola Bay. These 14 historical hurricanes provide a suite of varying storm characteristics that include track, landfall location, and intensity. We are not attempting to show how each hurricane would have looked in the past

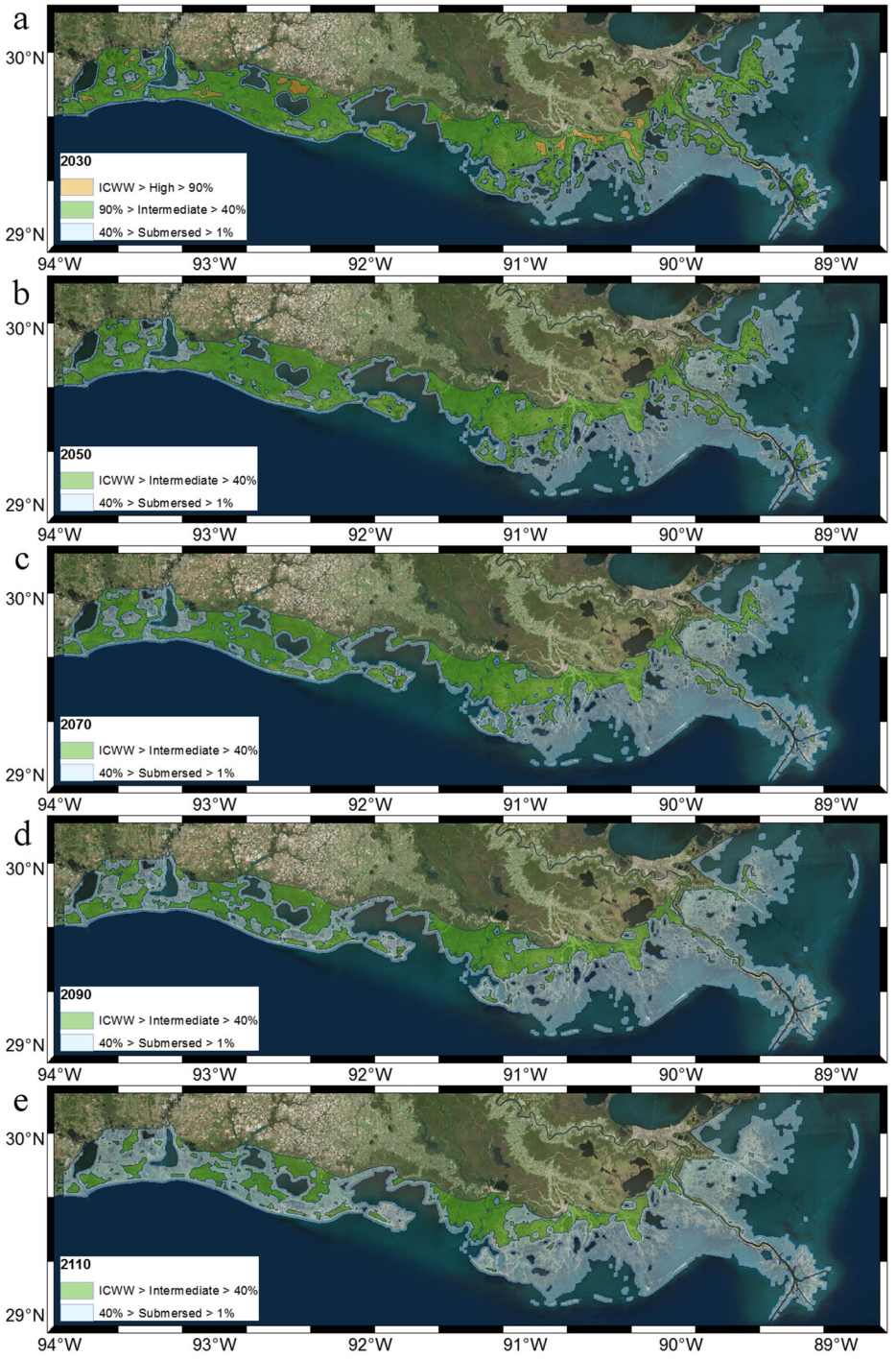

Fig. 3 Coastal zones high, intermediate, and submersed for **a** 2030, **b** 2050, **c** 2070, **d** 2090, and **e** 2110. Background: 2015/2016 satellite images. Storm surge models with navigation waterways and barrier islands are included in Online Resource 1

or may look in the future. Rather we are using the suite of storms to examine relative changes in storm surge characteristics between all eras. Outputs per mesh node include maximum water surface elevation, inundation time, current velocity, and wave statistics (Dietrich et al. 2011b). The maximum of maximums (MOM) water surface elevation is computed by finding the highest simulation output per node from all hurricanes. MOM water surface elevation differences are calculated by subtracting the earlier mesh year simulation output (i.e., 1850) from that of a later year (i.e., 2110).

3.5 Application of hydrologic coastal basins

Hydrologic coastal basins have been delineated across the Louisiana coast at least since the passage of the 1990 Coastal Wetlands Planning, Protection and Restoration Act (CWPPRA) (Barras et al. 2003; Boesch et al. 1994; Couvillion et al. 2011; Louisiana Coastal Wetlands Conservation and Restoration Task Force 1993; Twilley et al. 2016; Twilley et al. 2008; U.S. Army Corps of Engineers 2009). This analysis applies hydrologic unit code 6 (HUC6) coastal basins and the smaller HUC12 sub-watersheds, which fit within HUC6 coastal basins, as spatial bounds to quantify storm surge height and inundation time (Siverd et al. 2019; U.S. Geological Survey 2017a). Henceforth, HUC6 coastal basins are referred to as "coastal basins" while HUC12 sub-watersheds are referred to as "sub-watersheds."

4 Results

The following subsections include projections of future landscapes, a qualitative assessment of future landscapes, and detailed results concerning mean maximum of maximums (MOM) water surface elevations and maximum significant wave heights. For detailed results and discussion regarding inundation time and the impact of coastal deforestation, see Online Resource 1.

4.1 Qualitative assessment of future landscapes

Coastal zones high, intermediate, and submersed for 2030, 2050, 2070, 2090, and 2110 result from the previously discussed L:W isopleth inland migration trend from mesh year 1970 to 2010 (Fig. 3). South of Houma and Lafitte (Fig. 1a), the rate of inland migration of the 40% L:W isopleth visibly slows from 2070 to 2110 (Figs. 1c and 3) as the 40% isopleth encounters inland ridges and levees indicating near-total wetland loss by 2070 in this area. However, in southwest Louisiana between Sabine and Wax Lakes (Fig. 1b), negligible inland migration of the 40% isopleth occurs from 2030 to 2050 while substantial inland migration visibly occurs from 2070 to 2110.

Coastal zones high, intermediate, and submersed for 2050 and 2070 reveal substantial spatial similarities with previously published projections. The 2050 projection derived from this analysis and the 2040 projection created by the Louisiana Coastal Wetlands Conservation and Restoration Task Force (1993) demonstrate coast-wide similarity with our coastal zone intermediate (green) overlaying their wetland area (tan) and our coastal zone submersed (blue) overlaying their areas of open water (red). Specifically, white arrows point to the 40% L:W isopleth, which separates our intermediate and submersed coastal zones. In areas of disagreement, our analysis projects less future wetland loss southwest of Lafitte (yellow arrow) and

more wetland loss south of Lake Charles (red arrow) (Fig. 4a). For our same 2050 projection but versus the 2050 projection from Barras et al. (2003), similarity of future coastlines generally occurs across the coast. Our white intermediate zone generally overlays their green land areas and our blue submersed zone overlays their red land loss areas (black arrows point to the 40% L:W isopleth) except between the Biloxi Marsh and the east side of the Mississippi River (red arrow) (Fig. 4b). Notably, this area was substantially impacted by Hurricane Katrina in 2005 (Chen et al. 2008). The Louisiana Coastal Protection and Restoration Authority (2017) coastal master plan 2067 medium scenario for both no action (Fig. 4c) and with action (Fig. 4d) generally compares to our 2070 projection derived from this analysis. Agreement occurs where our intermediate coastal zone (green) overlays the land satellite image and where our coastal zone submersed (blue) overlays their areas of projected land loss (red). White arrows indicate areas of agreement while yellow arrows indicate areas of where the CPRA's projection is less optimistic than ours. The only area where we project more land loss is indicated by the red arrow (Fig. 4c). If the 2017 CPRA coastal masterplan is fully implemented, the comparison of our 2070 projection versus theirs is similar to that of without action except the areas of land gain (bright green) and areas that are maintained (brown) are included (Fig. 4d).

4.2 Storm surge evolution 1850–2010

Maximum surge output for all 14 storms is averaged across hydrologic coastal basins and called "mean maximum of maximums (MOM) water surface elevations" (Fig. 5). Mean MOM water surface elevations differences are quantified per sub-watersheds: 1890–1850 (Fig. 6(a)), 1930–1890 (Fig. 6(b)), and 2010–1930 (Fig. 6(c)). Mean MOM water surface elevation differences reveal little change from mesh year 1850 to 1890 across coastal Louisiana (Fig. 6(a), Table 2). Storm surge extends inland and is lower near the coast within coastal basins Atchafalaya-Vermilion, Terrebonne, and Barataria due to the loss of coastal forests by 1930 and GMSL rise (Fig. 6(b)). Storm surge is also able to propagate further up the Atchafalaya River in 1930 due to excavation of the Wax Lake Outlet, as illustrated by a 1.70-m difference within a sub-watershed in this area (Fig. 6(b), Table 3). Between 1930 and 2010, a smaller change of 0.26 m in mean MOM water surface elevations occurs within Atchafalaya-Vermilion while mean MOM changes of 0.34 m and 0.41 m occur across Terrebonne and Barataria, respectively (Fig. 6(c), Table 2). Sub-watershed statistics of Atchafalaya-Vermilion demonstrate trends different from those of Terrebonne and Barataria. For example, within Atchafalaya-Vermilion mean MOM water surface elevation difference, standard deviations are (m): 0.01, 0.26, 0.17, and 0.20 for 1890–1850, 1930–1890, 2010–1930, and 2110–2010 (Table 3). Mean MOM water surface elevation difference range also demonstrates a decrease in variability for 2010 minus 1930, 0.64 m, compared with 1930 minus 1890, 1.84 m, and 2110 minus 2010, 0.92 m, indicating the impact of maintained sediment input on the unfragmented landscape of Atchafalaya-Vermilion. For sediment-starved Terrebonne and Barataria, standard deviation and range consistently increase from the first interval of 1890 minus 1850 to the last interval of 2110 minus 2010.

Maximum significant wave height differences are quantified for each difference interval (Fig. 7). Similar to MOM water surface elevations, minimal change occurs from 1850 to 1890 in maximum significant wave heights. Relatively minor changes also occur from 1890 to 1930 except within the Lower Mississippi-New Orleans coastal basin where wave heights decrease due to the progradation of the Balize Delta (Fig. 7b). Similarly, wave heights decrease in the southeast area of the Atchafalaya-Vermilion coastal basin due to the emergence and growth of the Wax Lake-Atchafalaya Deltas from 1930 to 2010 (Fig. 7c).

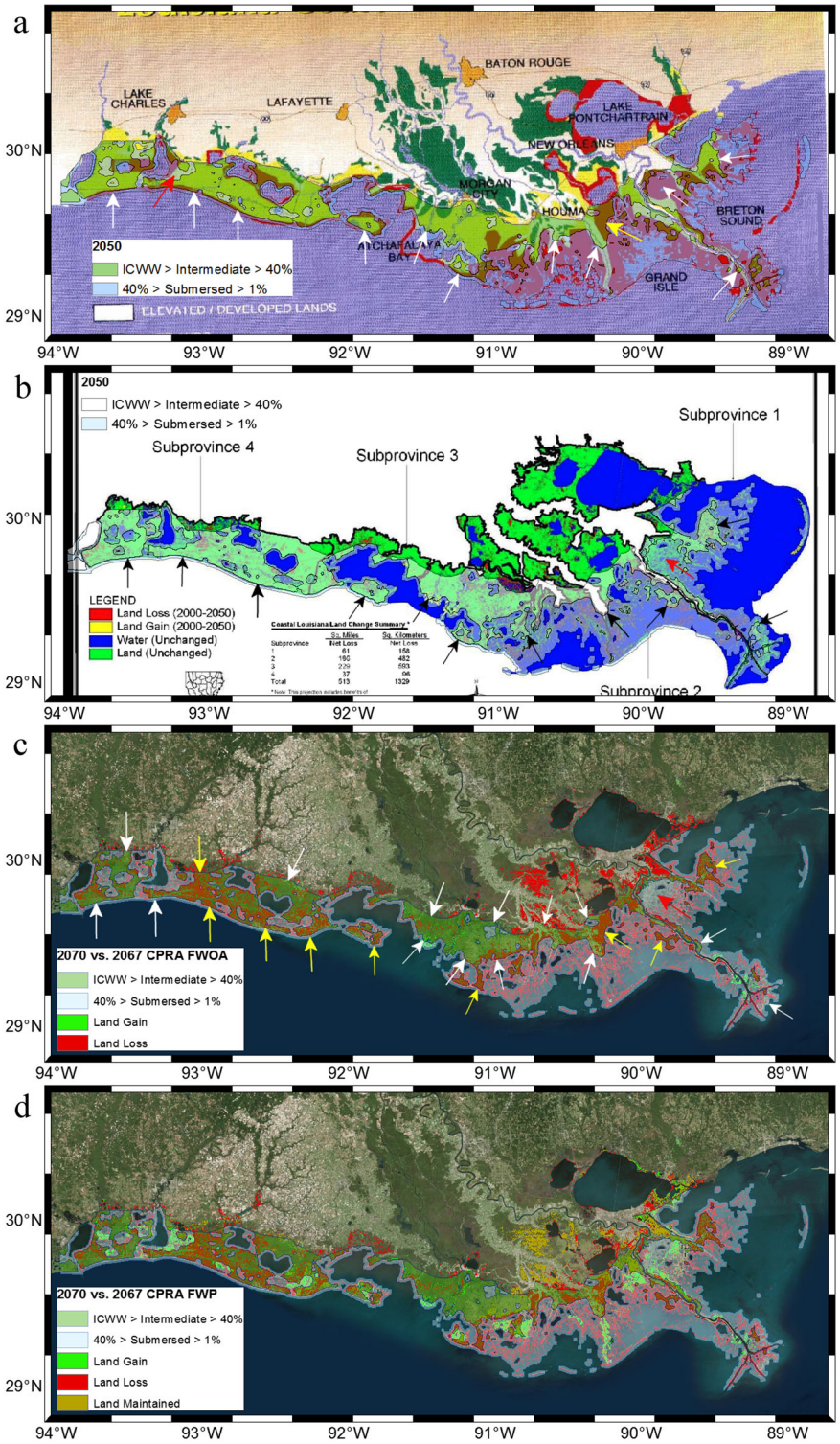

◀ **Fig. 4** Coastal zones versus projections of future Louisiana landscapes. **a** 2050 coastal zones versus Louisiana coastal landscape in 2040 (Louisiana Coastal Wetlands Conservation and Restoration Task Force 1993). Areas in red depict land loss by 2040 and are described as less than 50% land. **b** 2050 coastal zones versus USGS 2050 landscape (Barras et al. 2003). **c** 2070 coastal zones versus 2067 future without action-medium scenario. **d** 2070 versus 2067 future with action-medium scenario (Coastal Protection and Restoration Authority 2017). Similarity occurs where coastal zone intermediate (green) overlays the satellite image and submersed (blue) overlays areas of projected land loss (red)

4.3 Storm surge evolution 2010–2110

Mean MOM water surface elevation differences are quantified per sub-watersheds: 2110 minus 2010 (Fig. 6(d)) and 2110 minus 1850 (Fig. 6(e)). The contrast in changes in MOM water surface elevations across the three coastal basins Atchafalaya-Vermilion, Terrebonne, and

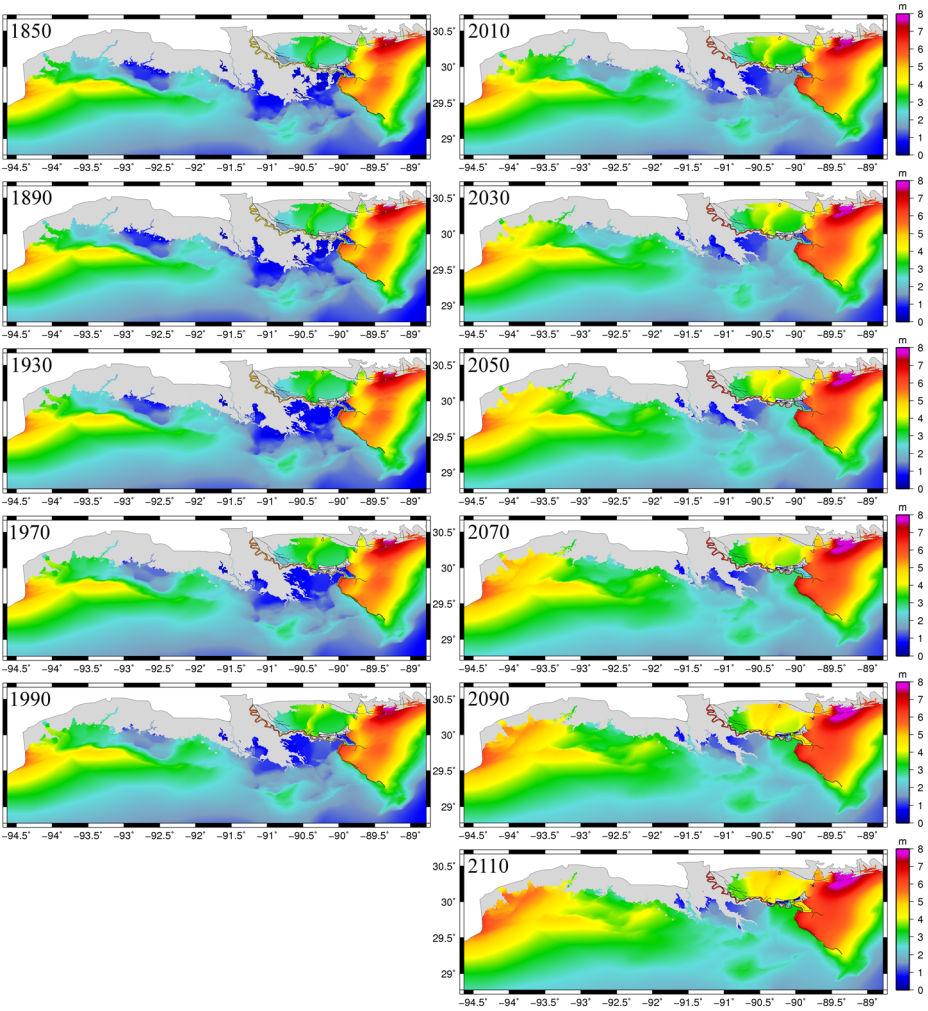

Fig. 5 Maximum of maximums (MOM) water surface elevations for all eleven storm surge model years from 1850 to 2110

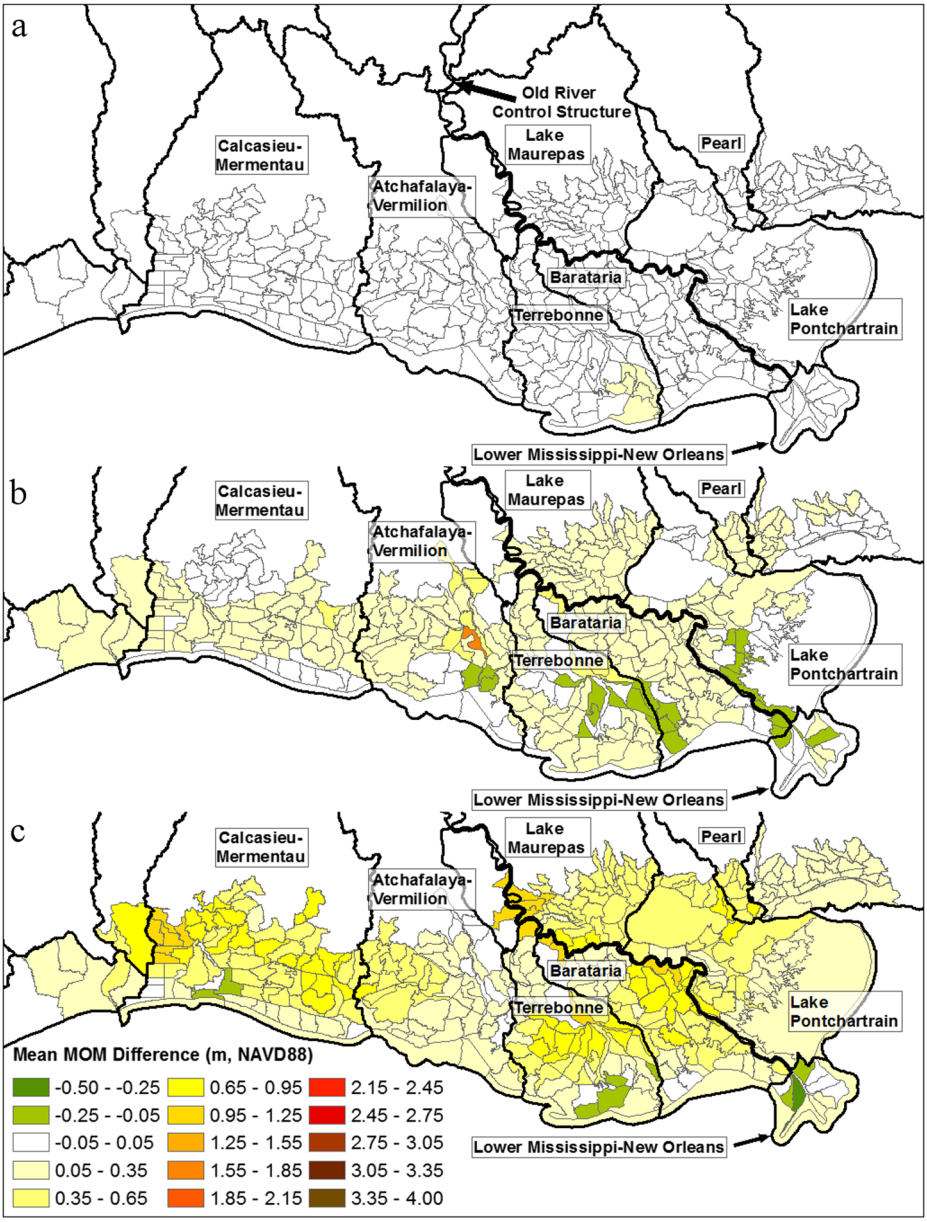

Fig. 6 Mean maximums of maximums (MOM) water surface elevations difference (m, NAVD88) per coastal basins (bold lines) and per sub-watersheds (gray lines) for: (a) 1890–1850, (b) 1930–1890, (c) 2010–1930, (d) 2110–2010, (e) 2110–1850. GMSL rise of 0.5 mm/year 1850–1890, 1 mm/year 1890–1930, 2 mm/year 1930–2010, 5.1 mm/year 2010–2110 is included

Barataria (0.67 m, 0.55 m, and 0.75 m, respectively) diminishes between 2010 and 2110 as the rate of annual GMSL rise increases (Fig. 6(d), Table 2). For sub-watersheds, standard deviation and range increase across the three coastal basins between 2010 and 2110 (Table 3), further indicating the impact of greater annual increases in future GMSL rise. Table 2 additionally

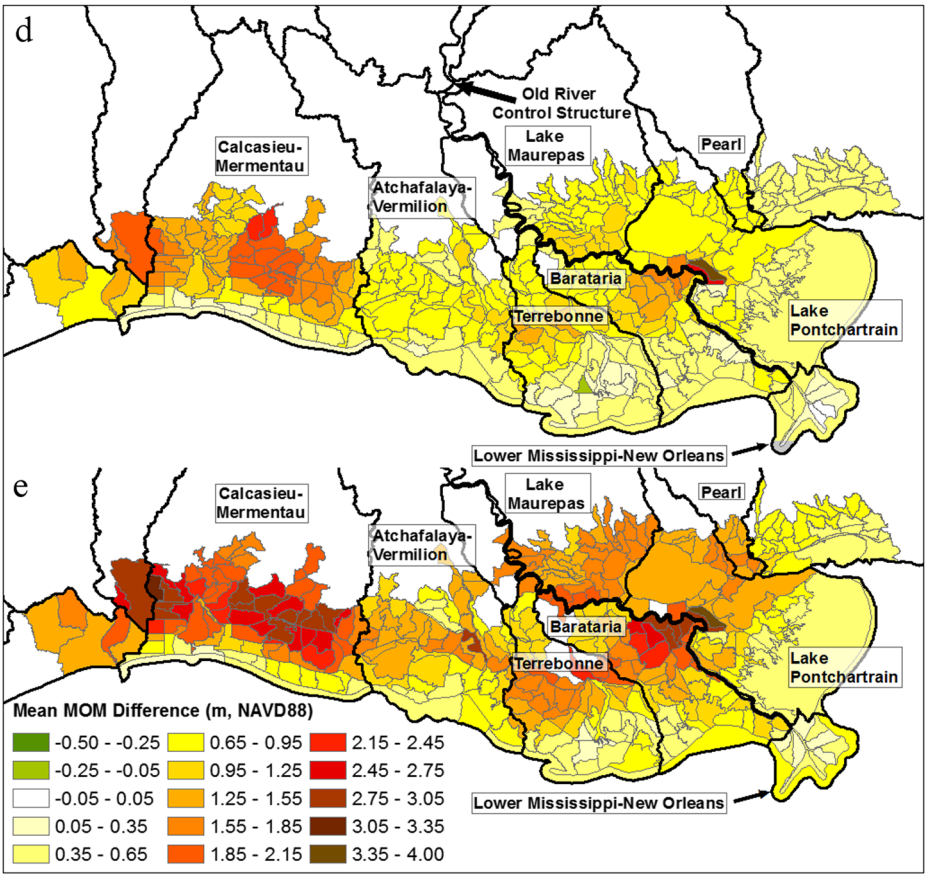

Fig. 6 (continued)

reveals the coastal basin with the smallest change in mean MOM water surface elevations from 2010 to 2110 is Lower Mississippi-New Orleans with an average increase of 0.39 m while Calcasieu-Mermentau experiences the greatest average increase, which is 1.15 m.

Between 2010 and 2110, all coastal basins except Lake Maurepas and Pearl feature an area where the difference in maximum significant wave heights exceeds 1 m. A large area within the Calcasieu-Mermenau coastal basin features wave height differences greater than 1 m due to substantial wetland loss by 2110 (Fig. 7d). In contrast with mesh year 1850, maximum significant wave heights increase more than 1 m by 2110 across coastal Louisiana due to both wetland loss and GMSL rise. A small exception occurs in the areas of Wax Lake-Atchafalaya delta growth (Fig. 7e).

5 Discussion

Sustainable land area (L) of a delta can be defined as the volumetric sediment discharge (Q_s) entering the delta multiplied by the fraction retained (f_r) and the volume contributed by organic

Table 2 Mean maximum of maximums (MOM) water surface elevations for all 14 hurricane storm surges (m). Mean MOM water surface elevations difference calculated by computing difference in 10 m × 10 m rasters and averaging across individual coastal basins. Coastal basins are sorted by smallest to largest mean MOM difference 2010–1930 (m). GMSL rise of 0.5 mm/year 1850–1890, 1 mm/year 1890–1930, 2 mm/year 1930–2010, 5.1 mm/year 2010–2110 is included

Mean maximum of maximums (MOM) water surface elevations (WSE) (m)

Coastal basin	Mean MOM WSE (m)					Mean MOM diff. (m)				
	1850	1890	1930	2010	2110	1890–1850	1930–1890	2010–1930	2110–2010	2110–1850
Lower Mississippi-New Orleans	2.72	2.74	2.78	2.85	3.24	0.02	0.04	0.07	0.39	0.52
Atchafalaya-Vermilion	2.14	2.16	2.22	2.47	3.05	0.02	0.08	0.26	0.67	1.02
Lake Pontchartrain	4.33	4.35	4.37	4.67	5.20	0.02	0.03	0.30	0.61	0.95
Terrebonne	1.58	1.61	1.65	1.95	2.50	0.03	0.08	0.34	0.55	0.95
Barataria	1.47	1.49	1.45	1.81	2.43	0.02	0.08	0.41	0.75	1.18
Calcasieu-Mermentau	2.47	2.48	2.57	2.94	4.03	0.02	0.10	0.43	1.15	1.64
Lake Maurepas	2.70	2.73	2.84	3.35	4.25	0.02	0.12	0.53	0.95	1.62
Pearl	4.65	4.67	4.74	5.30	6.02	0.02	0.07	0.61	0.79	1.50

Table 3 Sub-watershed statistics per coastal basin. Mean sub-watershed values calculated for MOM water surface elevation difference 10 m × 10 m rasters. GMSL rise of 0.5 mm/year 1850–1890, 1 mm/year 1890–1930, 2 mm/year 1930–2010, 5.1 mm/year 2010–2110 included

Sub-watershed statistics per coastal basin	MOM water surface elevation difference (m)				
	1890–1850 (Fig. 6a)	1930–1890 (Fig. 6b)	2010–1930 (Fig. 6c)	2110–2010 (Fig. 6d)	2110–1850 (Fig. 6e)
			Atchafalaya-Vermilion		
Mean	0.02	0.18	0.23	0.74	1.18
Median	0.02	0.08	0.22	0.77	1.20
Stand. dev.	0.01	0.26	0.17	0.20	0.41
Range	0.03	1.84	0.64	0.92	2.34
Minimum	0.00	− 0.14	0.01	0.30	0.54
Maximum	0.03	1.70	0.66	1.22	2.88
Count	55	55	55	56	55
			Terrebonne		
Mean	0.03	0.09	0.39	0.64	1.09
Median	0.02	0.09	0.32	0.59	1.04
Stand. dev.	0.02	0.14	0.32	0.35	0.54
Range	0.10	0.81	1.15	1.47	1.98
Minimum	0.00	− 0.21	− 0.06	− 0.08	0.24
Maximum	0.10	0.59	1.08	1.38	2.22
Count	54	54	55	58	54
			Barataria		
Mean	0.02	0.11	0.45	0.78	1.37
Median	0.02	0.10	0.40	0.74	1.16
Stand. dev.	0.02	0.14	0.27	0.36	0.63
Range	0.10	0.94	1.06	1.47	2.48
Minimum	0.00	− 0.49	− 0.03	0.20	0.36
Maximum	0.10	0.45	1.03	1.67	2.84
Count	55	55	56	57	55

production (r_0) divided by solids volume fraction (C_0) and relative sea level rise (sum of H and σ) (Paola et al. 2011):

$$L = \frac{Q_s f_r (1 + r_0)}{C_0 (\sigma + H)}$$

This equation for sustainable land area provides a lens to analyze the results of this study. Four distinct stages are established in the evolution of the coastal Louisiana landscape: (1) 1850–1890: minimal to no change in landscape; (2) 1890–1930: disappearance of the coastal forests and excavation of the Wax Lake Outlet; (3) 1930–2010: substantial wetland loss occurs in Terrebonne and Barataria coastal basins and emergence and growth of the Atchafalaya-Wax Lake Deltas within the Atchafalaya-Vermilion coastal basin; (4) 2010–2110: drowning of all coastal basins due to increased global mean sea level (GMSL) rise and continued subsidence. In terms of the Paola et al. (2011) equation, from 1850 to 2110, volumetric sediment discharge within the Mississippi River Delta decreases, while the annual rate of relative sea level rise increases. The result is reduced sustainable land area of the Mississippi River Delta, historical and future wetland collapse. Furthermore, because of the importance of riverine sediment inputs in delta growth and maintenance (Blum and Roberts 2009; Siverd et al. 2019), the assumed reduction in future delta growth and eventual retrogradation results in higher future

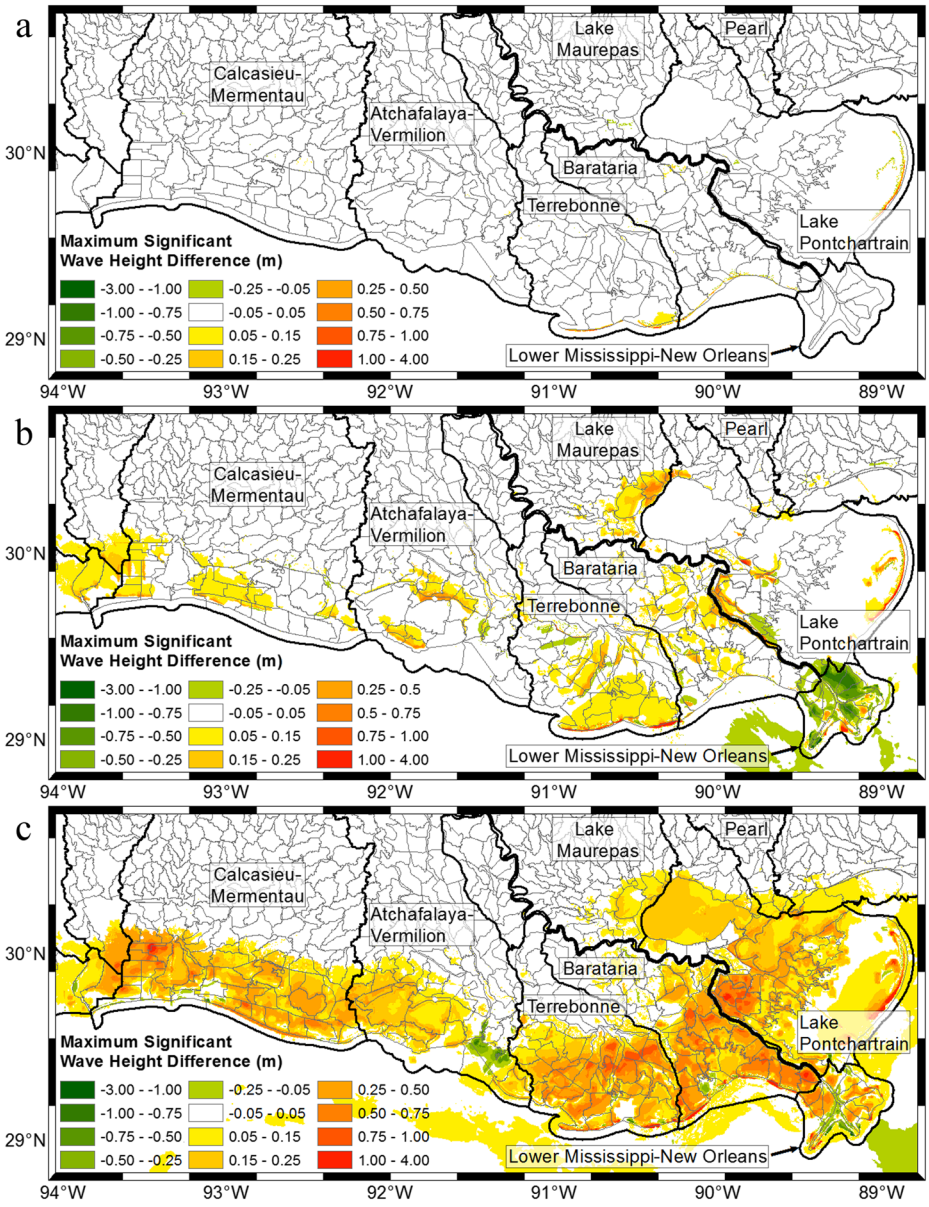

Fig. 7 10 m × 10-m maximum of maximums significant wave height difference plots. **a** 1890–1850. **b** 1930–1890. **c** 2010–1930. **d** 2110–2010. **e** 2110–1850. Coastal basins (bold lines) and sub-watersheds (gray lines) included for spatial reference. GMSL rise of 0.5 mm/year 1850–1890, 1 mm/year 1890–1930, 2 mm/year 1930–2010, 5.1 mm/year 2010–2110 is included. All subplots follow the same legend scale.

model surge output compared to if the Mississippi River Delta is supplied with sediment to compensate for relative sea level rise.

A comparative hurricane storm surge analysis for the period spanning 1850 to 2110 presents stark implications of the past and potential future evolution of the coastal Louisiana landscape. Water surface elevation differences correlate with changes in the Louisiana coastal

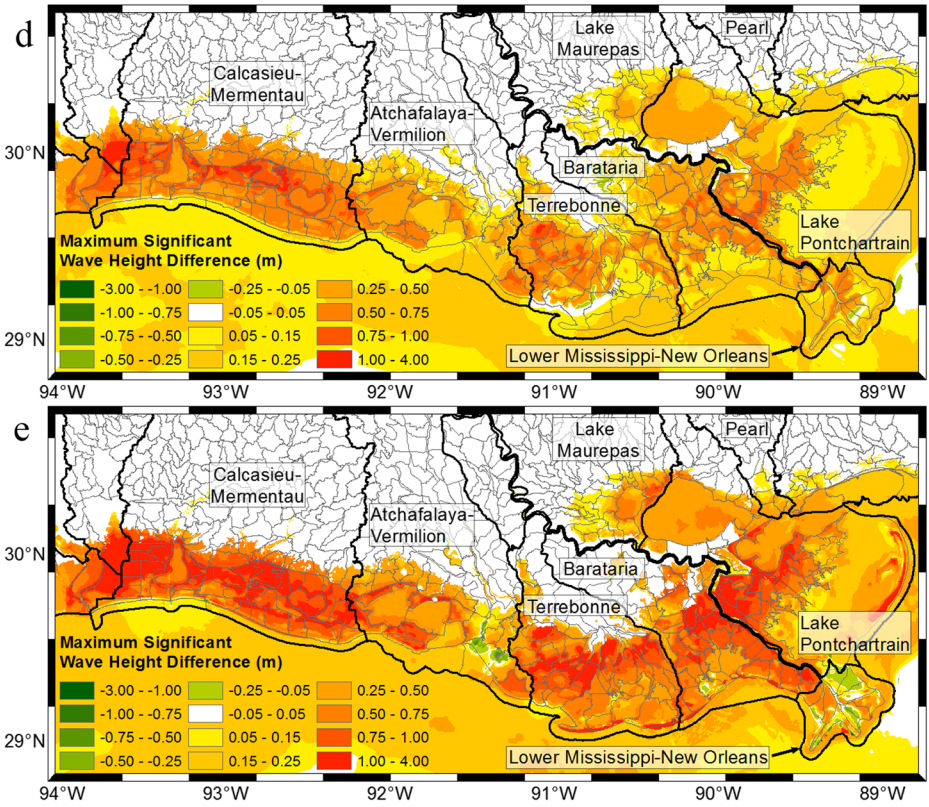

Fig. 7 (continued)

landscape. Minimal surge differences exist between 1850 and 1890. By 1930, storm surge propagates further inland due to the loss of coastal forests and excavation of the Wax Lake Outlet. Between 1930 and 2010, a smaller change of 0.26 m in maximum of maximums (MOM) water surface elevations occurs within Atchafalaya-Vermilion while changes of 0.34 m and 0.41 m occur within Terrebonne and Barataria, respectively. Mean MOM water surface elevations quantify the near uniform drowning of all three coastal basins between 2010 and 2110 via mean MOM differences of 0.67 m, 0.55 m, and 0.75 m for Atchafalaya-Vermilion, Terrebonne, and Barataria, respectively. All other coastal basins also drown with the greatest calculated mean MOM water surface elevation occurring in Calcasieu-Mermentau.

This analysis also confirms findings of past studies that suggest change in surge heights is nonlinear with GMSL rise (Atkinson et al. 2012; Bilskie et al. 2016a; Smith et al. 2010; Wamsley et al. 2010). For example, for mesh years 2010 through 2110, the Louisiana coastal landscape surrounding Lake Pontchartrain (Fig. 1a) is unaltered. However, the increase in mean maximum of maximums (MOM) water surface elevations within Lake Maurepas coastal basin sub-watersheds ranges 0.95–1.25 m from 2010 to 2110 while GMSL rise simulated during this period is only 0.51 m (Fig. 6(d)). The projected future increase in mean MOM water surface elevations within Lake Pontchartrain demonstrates the importance of the Biloxi Marsh and east Lake Pontchartrain land bridge in minimizing surge levels within the lake. Due

to the counter-clockwise rotation of hurricanes, future storm surge enters Lake Pontchartrain with less resistance as these two natural surge barriers deteriorate.

Changes in maximum significant wave heights are also nonlinear with greater differences occurring further inland in 2110 compared with 1850 (Fig. 7e). As interior wetlands between barrier islands and cities such as Houma continue to become more fragmented and deteriorate, waves propagate further inland until reaching resistance such as higher land or flood defenses. Because current flood defenses (levees, etc.) along the Louisiana coast are not designed for constant wave attack, future subsidence and GMSL rise will have major implications on flood protection. More robust and, therefore costlier, storm surge defenses will be required to maintain current levels of flood risk through 2110.

Future drowning of the Louisiana coastal landscape has major implications for similar deltas across the world, especially the Ganges, Irrawaddy, Magdalena, Mekong, Niger, and Tigris, which are subsiding faster than GMSL is rising. As noted in "Section 1," the Ganges and Mississippi Deltas feature similar areas less than 2 m above sea level and are historically impacted by storm surge and relative sea level rise rates (Syvitski et al. 2009). The Ganges and other similarly sinking deltas susceptible to storm surge will likely be impacted by higher inland surge heights similarly to the Mississippi River Delta. In addition, deltas no longer aggrading greater than relative sea level rise such as the Brahmani, Godavari, Indus, and Mahanadi (Syvitski et al. 2009) will also face similar challenges but on a longer time scale.

6 Conclusions

In this analysis, comparable representations of the Louisiana coastal landscape are developed for storm surge model mesh years 1850, 1890, 1930, 1970, 1990, 2010, 2030, 2050, 2070, 2090, and 2110 via historical maps for past landscapes. Projections of future landscapes are based on recent trends in landscape change and are comparable with projections of previous studies (Barras et al. 2003; Blum and Roberts 2009; Coastal Protection and Restoration Authority 2017; Dunbar et al. 1992; Gagliano et al. 1970; Louisiana Coastal Wetlands Conservation and Restoration Task Force 1993). A suite of historical storms is used to simulate storm surge and wind-waves for each mesh year. Surge output is averaged across hydrologic coastal basins and smaller sub-watersheds to quantify and evaluate surge evolution.

From 1930 to 2010, mean maximum water surface elevations within the sediment-starved Terrebonne and Barataria coastal basins are multiples of 1.3 and 1.6 greater than those of sediment abundant Atchafalaya-Vermilion. However, from 2010 to 2110, differences in mean maximum water surface elevations across Atchafalaya-Vermilion, Terrebonne, and Barataria are 0.67 m, 0.55 m, and 0.75 m, respectively, revealing little future distinction among these three coastal basins. Mean maximum significant wave heights also indicate little differentiation among these coastal basins from 2010 to 2110. By 2110, increases in inland surge heights double the applied sea level rise along the shore of Lake Pontchartrain and in southwest Louisiana indicating a nonlinear relationship between storm surge and GMSL rise. A rapid rate of annual GMSL rise during the twenty-first century would therefore have major implications for future flood exposure and associated flood defense costs across coastal Louisiana (Kulp and Strauss 2017; Wong et al. 2017).

Throughout the twenty-first century, the Mississippi Delta will experience extensive drowning due to a rate of relative sea level rise that is substantially greater than the rate of aggradation. In contrast, historical changes in the Louisiana coastal landscape resulted from

local anthropogenic influences such as changes in Mississippi River management. The results of this analysis have major implications for similar deltas across the world. As the rate of annual relative sea level rise increases, deltas susceptible to storm surge will experience increased inland surge heights to the detriment of local inhabitants and ecosystems. However, establishing recent landscape and storm surge evolution trends of major coastal deltas and projecting these trends beyond 50 years into the future could aide policy makers as they work to enhance resilience.

Acknowledgments This work also used high-performance computing at Louisiana State University (LSU) and the Louisiana Optical Network Initiative (LONI).

Funding information This research was supported by the Coastal SEES program of the National Science Foundation (NSF) (EAR-1533979 and EAR-1427389), the Louisiana Sea Grant Laborde Chair, and the Louisiana Geological Survey.

Compliance with ethical standards

Disclaimer The statements and conclusions are those of the authors and do not necessarily reflect the views of NSF, Louisiana Sea Grant, LSU, or LONI. This work used the Extreme Science and Engineering Discovery Environment (XSEDE), which is supported by the National Science Foundation (NSF) grant ACI-1053575. This publication also made use of data sets provided by the Coastal Protection and Restoration Authority (CPRA) which were originally produced to inform the development of the 2017 Coastal Master Plan. To implement coastal forests for mesh years 1850 and 1890, this publication made use of digitized maps of coastal Louisiana provided by the Williams Research Center of the Historic New Orleans Collection located in New Orleans, LA.

Conflict of interest The authors declare that they have no conflict of interest.

References

Ali A (1999) Climate change impacts and adaptation assessment in Bangladesh. Climate Res 12:109–116. https://doi.org/10.3354/cr012109

Atkinson J, McKee Smith J, Bender C (2012) Sea-level rise effects on storm surge and nearshore waves on the Texas coast: influence of landscape and storm characteristics Journal of Waterway. Port, Coastal, and Ocean Engineering 139:98–117

Barras J et al. (2003) Historical and projected coastal Louisiana land changes: 1978-2050 vol 03. U.S. Geological Survey

Batker D, de la Torre I, Costanza R, Swedeen P, Day J, Boumans R, Bagstad K (2010) Gaining ground: wetlands, hurricanes, and the economy: the value of restoring the Mississippi River Delta. Institute for Sustainable Solutions, Earth Economics

Bilskie MV, Hagen SC (2013) Topographic accuracy assessment of bare earth lidar-derived unstructured meshes. Adv Water Resour 52:165–177. https://doi.org/10.1016/j.advwatres.2012.09.003

Bilskie MV, Hagen SC, Medeiros SC, Passeri DL (2014) Dynamics of sea level rise and coastal flooding on a changing landscape. Geophys Res Lett 41:927–934. https://doi.org/10.1002/2013gl058759

Bilskie MV, Coggin D, Hagen SC, Medeiros SC (2015) Terrain-driven unstructured mesh development through semi-automatic vertical feature extraction. Adv Water Resour 86:102–118. https://doi.org/10.1016/j.advwatres.2015.09.020

Bilskie MV, Hagen SC, Alizad K, Medeiros SC, Passeri DL, Needham HF, Cox A (2016a) Dynamic simulation and numerical analysis of hurricane storm surge under sea level rise with geoomorphic changes along the northern Gulf of Mexico. Earth's Future 4:177–193

Bilskie MV, Hagen SC, Medeiros SC, Cox AT, Salisbury M, Coggin D (2016b) Data and numerical analysis of astronomic tides, wind-waves, and hurricane storm surge along the northern Gulf of Mexico. J Geophys Res-Oceans 121:3625–3658. https://doi.org/10.1002/2015jc011400

Bilskie MV, Hagen SC, Irish JL (2019) Development of return period stillwater floodplains for the northern Gulf of Mexico under the coastal dynamics of sea level rise. J Waterw Port Coast 145:04019001. https://doi.org/10.1061/(Asce)Ww.1943-5460.0000468

Blain CA, Westerink JJ, Luettich RA (1998) Grid convergence studies for the prediction of hurricane storm surge. Int J Numer Methods Fluids 26:369–401. https://doi.org/10.1002/(Sici)1097-0363(19980228)26:4<369::Aid-Fld624>3.0.Co;2-0

Blum MD, Roberts HH (2009) Drowning of the Mississippi Delta due to insufficient sediment supply and global sea-level rise. Nat Geosci 2:488–491. https://doi.org/10.1038/ngeo553

Boesch DF, Josselyn MN, Mehta AJ, Morris JT, Nuttle WK, Simenstad CA, Swift DJ (1994) Scientific assessment of coastal wetland loss, restoration and management in Louisiana. Journal of Coastal Research:i-103

Booij N, Ris RC, Holthuijsen LH (1999) A third-generation wave model for coastal regions-1. Model description and validation. J Geophys Res-Oceans 104:7649–7666. https://doi.org/10.1029/98jc02622

Chen Q, Wang LX, Tawes R (2008) Hydrodynamic response of northeastern Gulf of Mexico to hurricanes. Estuar Coasts 31:1098–1116. https://doi.org/10.1007/s12237-008-9089-9

Church JA et al (2013) Sea level change. Cambridge University Press, Cambridge, United Kingdom and New York, NY, USA

Coastal Protection and Restoration Authority (2017) Louisiana's comprehensive master plan for a sustainable coast. CPRA, Baton Rouge, LA

Coastal Protection, Restoration Authority (2018) Barrier island status report: fiscal year 2020 Annual Plan. Rouge, Baton

Conner WH, Toliver JR (1990) Long-term trends in the bald-cypress (Taxodium distichum) resource in Louisiana (U.S.A.). For Ecol Manag 33-34:543–557. https://doi.org/10.1016/0378-1127(90)90217-y

Couvillion BR et al. (2011) Land area change in coastal Louisiana from 1932 to 2010. U.S. department of the Interior: U.S. Geological Survey Scientific Investigations Map 3164, scale 1:265,000, Reston, Virginia

Cox AT, Greenwood JA, Cardone VJ, Swail VR (1995) An interactive objective kinematic analysis system. Alberta, Canada

Day JW Jr et al (2007) Restoration of the Mississippi Delta: lessons from Hurricanes Katrina and Rita. Science 315:1679–1684. https://doi.org/10.1126/science.1137030

Day JW, Kemp GP, Reed DJ, Cahoon DR, Boumans RM, Suhayda JM, Gambrell R (2011) Vegetation death and rapid loss of surface elevation in two contrasting Mississippi delta salt marshes: the role of sedimentation, autocompaction and sea-level rise. Ecol Eng 37:229–240. https://doi.org/10.1016/j.ecoleng.2010.11.021

Dietrich JC, Tanaka S, Westerink JJ, Dawson CN, Luettich RA Jr, Zijlema M, Westerink HJ (2011a) Performance of the unstructured-mesh, SWAN+ADCIRC model in computing hurricane waves and surge. J Sci Comput 52:468–487

Dietrich JC et al (2011b) Modeling hurricane waves and storm surge using integrally-coupled, scalable computations. Coast Eng 58:45–65. https://doi.org/10.1016/j.coastaleng.2010.08.001

Dunbar JB, Britsch LD, Kemp EB (1992) Land loss rates. Report 3. Louisiana Coastal Plain (No. WES/TR/GL/90-2). Army Engineer Waterways Experiment Station Geotechnical Lab, Vicksburg, MS

Fischbach JR et al (2017) 2017 Coastal master plan modeling: attachment C3-25: storm surge and risk assessment. Final Version, Coastal Protection and Restoration Authority, Baton Rouge, LA

Gagliano SM, Kwon HJ, Van Beek JL (1970) Deterioration and restoration of coastal wetlands. Coastal Engineering Proceedings 1:1767–1782

Harrison R (2015) Impact of the Gulf Intracoastal Waterway (giww) on freight flows in the Texas-Louisiana mega region

Irish JL, Sleath A, Cialone MA, Knutson TR, Jensen RE (2013) Simulations of Hurricane Katrina (2005) under sea level and climate conditions for 1900. Clim Chang 122:635–649

Jevrejeva S, Jackson LP, Riva RE, Grinsted A, Moore JC (2016) Coastal sea level rise with warming above 2 degrees C. Proc Natl Acad Sci U S A 113:13342–13347. https://doi.org/10.1073/pnas.1605312113

Kulp S, Strauss BH (2017) Rapid escalation of coastal flood exposure in US municipalities from sea level rise. Clim Chang 142:477–489. https://doi.org/10.1007/s10584-017-1963-7

Lawler S, Haddad J, Ferreira CM (2016) Sensitivity considerations and the impact of spatial scaling for storm surge modeling in wetlands of the Mid-Atlantic region. Ocean Coast Manage 134:226–238. https://doi.org/10.1016/j.ocecoaman.2016.10.008

Louisiana Coastal Wetlands Conservation and Restoration Task Force (1993) Louisiana coastal wetlands restoration plan: main report and environmental impact statement. Louisiana State University, Baton Rouge, Louisiana

Luettich Jr. RA, Westerink JJ, Scheffner NW (1992) ADCIRC: an advanced three-dimensional circulation model for shelves, coasts and estuaries vol DRP-92-6. U.S. Army Corps of Engineers, ERDC-ITL-K, 3909 Halls Ferry Rd., Vicksburg, MS 39180-6199

Luettich R, Westerink J (2004) Formulation and numerical implementation of the 2D/3D ADCIRC finite element model version 44.XX:74

Massey TC, Wamsley TV, Cialone MA (2011) Coastal storm modeling-system integration solutions to coastal disasters 2011:99-108

Massey TC, Ratcliff JJ, Cialone MA (2015) North Atlantic Coast Comprehensive Study (NACCS) storm simulation and statistical analysis: part II-high performance semi-automated production system. The Proceedings of the Coastal Sediments 2015

National Oceanic and Atmospheric Administration (2018) Tides and currents. Center for Operational Oceanographic Products and Services. https://tidesandcurrents.noaa.gov/. Accessed 3/4/2018 2018

Nienhuis JH, Tornqvist TE, Jankowski KL, Fernandes AM, Keogh ME (2017) A new subsidence map for coastal Louisiana GSA Today 27

Paola C et al (2011) Natural processes in delta restoration: application to the Mississippi Delta. Ann Rev Mar Sci 3:67–91. https://doi.org/10.1146/annurev-marine-120709-142856

Powell MD, Houston SH, Amat LR, Morisseau-Leroy N (1998) The HRD real-time hurricane wind analysis system. Journal of Wind Engineering and Industrial Aerodynamics 77-8:53–64. https://doi.org/10.1016/S0167-6105(98)00131-7

Resio DT, Westerink JJ (2008) Modeling the physics of storm surges. Phys Today 61:33–38. https://doi.org/10.1063/1.2982120

Siverd CG, Hagen SC, Bilskie MV, Braud DH, Peele RH, Twilley RR (2018) Hydrodynamic storm surge model simplification via application of land to water isopleths in coastal Louisiana. Coast Eng 137:28–42. https://doi.org/10.1016/j.coastaleng.2018.03.006

Siverd CG, Hagen SC, Bilskie MV, Braud DH, Gao S, Peele RH, Twilley RR (2019) Assessment of the temporal evolution of storm surge across coastal Louisiana. Coast Eng 150:59–78. https://doi.org/10.1016/j.coastaleng.2019.04.010

Smith JM, Cialone MA, Wamsley TV, McAlpin TO (2010) Potential impact of sea level rise on coastal surges in southeast Louisiana. Ocean Eng 37:37–47. https://doi.org/10.1016/j.oceaneng.2009.07.008

Stocker TF et al. (2013) Intergovernmental panel on climate change, working group I contribution to the IPCC fifth assessment report (AR5).

Sweet WV, Kopp RE, Weaver CP, Obeyesekera J, Horton RM, Thieler ER, Zervas C (2017) Global and regional sea level rise scenarios for the United States. National Oceanic and Atmospheric Administration. Silver Spring, Maryland

Syvitski JPM et al (2009) Sinking deltas due to human activities. Nat Geosci 2:681–686. https://doi.org/10.1038/Ngeo629

Turner RE, McClenachan G (2018) Reversing wetland death from 35,000 cuts: opportunities to restore Louisiana's dredged canals. PloS one 13:e0207717

Twilley RR, Couvillion BR, Hossain I, Kaiser C, Owens AB, Steyer GD, Visser JM (2008) Coastal Louisiana Ecosystem Assessment and Restoration Program: the role of ecosystem forecasting in evaluating restoration planning in the Mississippi River Deltaic Plain. Am Fish Soc Symp 64:29–46

Twilley RR et al (2016) Co-evolution of wetland landscapes, flooding, and human settlement in the Mississippi River Delta. Plain Sustain Sci 11:711–731. https://doi.org/10.1007/s11625-016-0374-4

U.S. Army Corps of Engineers (2008) Louisiana coastal protection and restoration technical report. USACE, Vicksburg, Mississippi

U.S. Army Corps of Engineers (2009) Louisiana coastal protection and restoration (LACPR) final technical report. New Orleans District, New Orleans, LA

U.S. Army Corps of Engineers (2016) The Mississippi River. U.S. Army Corps of Engineers. http://www.mvn.usace.army.mil/Missions/Mississippi-River-Flood-Control/Mississippi-River-Tributaries/. Accessed 12/8/2017 2017

U.S. Geological Survey (2017a) Hydrologic Unit Maps. U.S. Department of the Interior. https://water.usgs.gov/GIS/huc.html. Accessed 7/11/2018 2018

U.S. Geological Survey (2017b) Topoview. U.S. Department of the Interior. https://ngmdb.usgs.gov/topoview/viewer/#4/40.01/-100.06. Accessed 12-27-2017

Ulm M, Arns A, Wahl T, Meyers SD, Luther ME, Jensen J (2016) The impact of a Barrier Island loss on extreme events in the Tampa Bay. Front Mar Sci 3

Vörösmarty CJ, Syvitski J, Day J, De Sherbinin A, Giosan L, Paola C (2009) Battling to save the world's river deltas. Bulletin of the Atomic Scientists 65:31–43

Walstra DJ, de Vroeg J, de Vries JVT, Swinkels C, Luijendijk A, de Boer W, Dekker F (2012) A comprehensive sediment budget for the Mississippi barrier islands. Coastal Engineering Proceedings 1:81

Wamsley TV, Cialone MA, Smith JM, Atkinson JH, Rosati JD (2010) The potential of wetlands in reducing storm surge. Ocean Eng 37:59–68. https://doi.org/10.1016/j.oceaneng.2009.07.018

Wells JT, Chinburg SJ, Coleman JM (1984) Development of Atchafalaya River deltas: generic analysis. U.S. Army Corps of Engineers, Vicksburg, MS

Westerink JJ et al (2008) A basin- to channel-scale unstructured grid hurricane storm surge model applied to southern Louisiana Monthly Weather Review 136:833-864. https://doi.org/10.1175/2007mwr1946.1

Wong TE, Bakker AMR, Keller K (2017) Impacts of Antarctic fast dynamics on sea-level projections and coastal flood defense. Clim Chang 144:347–364. https://doi.org/10.1007/s10584-017-2039-4

Zijlema M (2010) Computation of wind-wave spectra in coastal waters with SWAN on unstructured grids. Coast Eng 57:267–277. https://doi.org/10.1016/j.coastaleng.2009.10.011

Affiliations

Christopher G. Siverd[1] · Scott C. Hagen[1,2,3,4] · Matthew V. Bilskie[2] · DeWitt H. Braud[4] · R. Hampton Peele[5] · Madeline R. Foster-Martinez[2] · Robert R. Twilley[4,6]

Scott C. Hagen
shagen@lsu.edu

Matthew V. Bilskie
mbilsk3@lsu.edu

DeWitt H. Braud
dbraud1@lsu.edu

R. Hampton Peele
hampton@lsu.edu

Madeline R. Foster-Martinez
mrfoster@uno.edu

Robert R. Twilley
rtwilley@lsu.edu

[1] Department of Civil and Environmental Engineering, Louisiana State University, 3255 Patrick F. Taylor, Baton Rouge, LA 70803, USA

[2] Center for Coastal Resiliency, Louisiana State University, 124C Sea Grant Building, Baton Rouge, LA 70803, USA

[3] Center for Computation and Technology, Louisiana State University, 340 E. Parker Blvd, Baton Rouge, LA 70803, USA

[4] Coastal Studies Institute, Louisiana State University, Howe-Russell Geoscience Complex, Room 331, Baton Rouge, LA 70803, USA

[5] Louisiana Geological Survey, Louisiana State University, 3079 Energy, Coastal and Environment Building, Baton Rouge, LA 70803, USA

[6] College of Coast and Environment, Louisiana State University, 1002-Q Energy, Coastal and Environment Building, Baton Rouge, LA 70803, USA